

THE PERFORMANCE OF TRANSIT TIME FLOWMETERS IN HEATED GAS MIXTURES

John D. Wright
Process Measurement Division
Chemical Science and Technology Laboratory
National Institute of Standards and Technology
Gaithersburg, Maryland 20899-0001 USA
email: john.wright@nist.gov

ABSTRACT

An ultrasonic transit time flowmeter was tested over Reynolds numbers from 1000 to 100 000 in a calibration facility that generates gas flows with controlled temperature and composition. The gas mixtures were composed of air, nitrogen, carbon dioxide, water vapor, and argon, and the mixture temperature ranged from 290 K to 450 K. The test program was conducted to determine the sensitivity of the flowmeter output to gas composition and temperature and to find the appropriate dimensionless quantities for the presentation of calibration results. Plots of discharge coefficient versus Reynolds number collapse the data well for all of the conditions tested. Comparisons between the experimentally measured discharge coefficients and those predicted by computer models using postulated velocity profiles are presented, and they show good qualitative agreement. The effects of thermal expansion on sound path length and pipe diameter were significant over the tested temperature range.

NOMENCLATURE

A	Cross sectional area of pipe
c	Sound speed
C_d	Discharge coefficient
k_T	Path length thermal correction
\dot{m}	Reference mass flow
t_{up}, t_{dn}	Transit times up and downstream
V_ℓ	Path mean velocity (of the fluid)
V_B	Bulk mean velocity (of the fluid)
ℓ	Length of the sound path
ϕ	Angle of sound path

ρ	Gas density
α	Thermal expansion coefficient
subscripts and superscripts	
H	Handbook value
m	Meter value
0	Reference temperature condition
T	Actual temperature condition

INTRODUCTION

In recent years, ultrasonic transit time flowmeters designed for use in gas flows have become commercially available. These meters have good accuracy, do not obstruct the flow (or lead to any significant pressure losses), and have a wide flow rangeability (100 to 1 or more). Transit time flowmeters are good candidates for the measurement of gas mixtures that vary in temperature and composition, such as vehicle exhaust, the exhaust from furnaces, or humid air.

PRINCIPLE OF OPERATION

An ultrasonic transit time flowmeter uses two ultrasonic transducers to transmit sound pulses alternately upstream and downstream through the flow (Lynnworth, 1989, Brown, 1991). The times required for the sound to travel in the opposite directions can be used to calculate both the sound speed and the mean fluid velocity along the path followed by the sound ("path mean velocity"). The acoustic transducers are generally positioned flush with the inner surface of the pipe wall and at an angle to the pipe axis (ϕ). The reflective

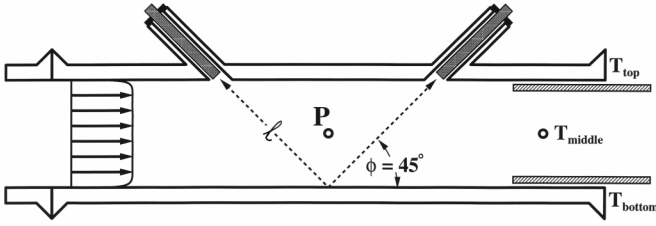


Figure 1. The arrangement of ultrasonic, pressure, and temperature sensors in the tested transit time flowmeter.

arrangement used in the present test is shown in Fig. 1.

For the transit time flowmeter, assuming only axial velocity components, the governing equations are:

$$V_\ell = \frac{\ell}{2 \cdot \cos(\phi)} \cdot \left(\frac{1}{t_{dn}} - \frac{1}{t_{up}} \right), \quad (1)$$

$$c = \frac{\ell}{2} \cdot \left(\frac{1}{t_{dn}} + \frac{1}{t_{up}} \right). \quad (2)$$

The path mean velocity (V_ℓ) may be multiplied by a discharge coefficient (C_d) to obtain a value for the bulk mean velocity (V_B),

$$V_B = C_d \cdot V_\ell. \quad (3)$$

The value of the discharge coefficient varies with flow due to changes in the velocity profile shape, but often, meter manufacturers choose a range of flows over which the meter is designed to operate and assume that the discharge coefficient is a constant over this range. The changes in velocity profile shape which cause variation in the discharge coefficient and also the transition from laminar to turbulent flow are functions of the Reynolds number. Based on the understanding of the influence quantities for a transit time flowmeter and dimensional analysis, a plot of discharge coefficient versus Reynolds number is an appropriate way to present calibration data. This method of presentation should “collapse” the

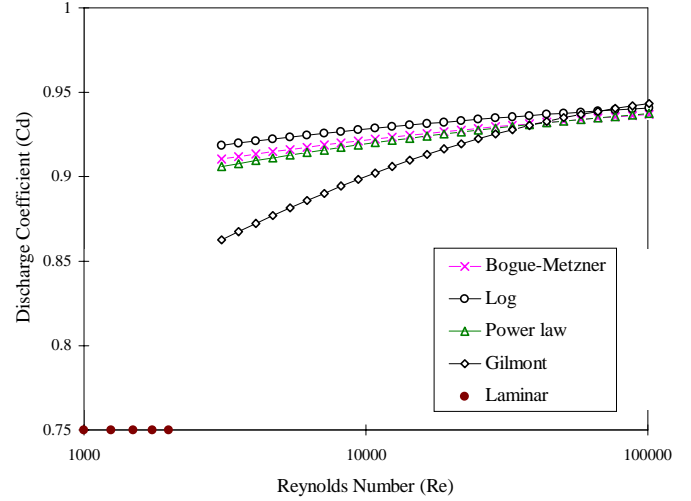


Figure 2. Transit time flowmeter discharge coefficients versus Reynolds number for various analytical velocity profile functions.

calibration data from various operating conditions to a single calibration curve, and is the most robust and convenient approach for predicting the necessary discharge coefficient for some new, untested operating condition.

Yeh and Mattingly (1997), Lynnworth (1989), and Brown (1991) have postulated certain analytical velocity profile functions available in the literature and computed predictions of the effects of Reynolds number on the discharge coefficient of a single path transit time flowmeter. A version of such a prediction is presented in Fig. 2. Discharge curves for the Bogue and Metzner (1963) profile, log function profile, power law, and Gilmont (1996) profile are shown. The parabolic velocity profile from Poiseuille flow gives a constant discharge coefficient of 0.75 for laminar flow ($Re < 2000$). For $2000 < Re < \approx 3000$ (the transition region) the flow is intermittently laminar and turbulent and the available analytical velocity profile functions are not deemed reliable for discharge coefficient predictions.

One motivation for the experimental study of the transit time flowmeter in heated gas mixtures was to validate, over a wide range of conditions, that Re and C_d are appropriate quantities for the presentation and extrapolation of meter calibration data. Further goals were to shed light on the behavior of the discharge coefficient in the transition region and to ascertain which analytical profile functions are best suited for discharge coefficient predictions, particularly at Reynolds numbers below 30 000 where the differences between the analytical functions are most pronounced.

EXPERIMENT DESCRIPTION

A transit time flowmeter with high temperature ultrasonic transducers operating at 50 MHz was installed in a horizontal flow tube. The sound was reflected off the far wall of the pipe between the transducers with a 45° path. The inside diameter of the 316 stainless steel flow tube was 7.74 cm, and the flow tube was 49 cm long. For most of the tests, the meter was oriented so that the sound path fell in a vertical plane (transducers on top of the flow tube). A pressure tap was located on the side wall at the flowmeter centerline (i.e., half way between the two transducers, see Fig. 1). A temperature tap was located 20 cm downstream from the flowmeter centerline, and a resistance temperature device (RTD) was inserted into the flow tube. The outlet of the flow tube discharged to the room which was maintained at 292 K ± 2 K. Two more RTD's were inserted into the flow tube exit so that they were 14.7 cm downstream from the flowmeter centerline (see Fig. 1). One of these RTD's was 0.4 cm from the crown of the flow tube while the other was 0.4 cm from the bottom. These two RTD's permitted the measurement of temperature differences between the top and bottom of the flow. The flow tube was wrapped with 2.5 cm thick fiberglass insulation. Upstream from the flow tube was an approach pipe of the same inside diameter, 60 pipe diameters long, and the joint connecting the flow tube and approach pipe was smooth. The approach pipe was heated and insulated. A proportional-integral-derivative controller with the set point equal to the temperature of the flowing gas set point was used to control the approach pipe heaters.

The known flows were generated with the NIST Heated Gas Mixture Flow Facility (HGMFF). The details of the facility design and an uncertainty analysis of the mass flow measurement have been described in an earlier publication (Wright and Espina, 1997). The facility meters pure air, nitrogen, carbon dioxide, and argon with critical flow nozzles that have been calibrated using established NIST gas flow standards (piston and bell provers). Water vapor is added in a saturator vessel and the mass flow of water is calculated from a dew point temperature measurement. The metered gas mixture can be heated by an electric circulation heater to temperatures between 292 K and 700 K. The flow range of the facility is nominally (60 to 6000) standard L / min (slm)¹ for air and (60 to 2000) slm for simulated exhaust mixtures.

The set point conditions established for the flowmeter test were designed to cover a wide range of flows and gas properties (i.e., density, viscosity, and composition). The flow set points were: (80, 140, 280, 430, 560, 1100, 1700, 2300, 2800, 3500, 4200, and 5000) slm. The temperature and composition conditions were: (1) humid air (12 %² H₂O and 88 % air) at 394 K, (2) simulated exhaust (13.5 % CO₂, 12 % H₂O, 0.9 % Ar, and 73.6 % N₂) at 394 K, (3) dry air at 444 K, (4) dry air at 394 K, (5)

dry air at 344 K, and (6) dry air at 292 K. After each set point change, conditions were allowed to stabilize for 5 minutes or more before data collection commenced. For each test, two sets of five, thirty second averages were collected at each flow set point, cycling through the flows in decreasing, then increasing order.

UNCERTAINTY OF THE BULK MEAN VELOCITY

For the transit time flowmeter evaluation, it was necessary to calculate the bulk mean velocity of the flow at the meter test section, via the following equation,

$$V_B = \frac{\dot{m}}{\rho \cdot A} \quad (4)$$

The HGMFF measures mass flow with a relative expanded uncertainty of 1 % of reading or less (Wright and Espina, 1997).³ Uncertainty in the pipe cross sectional area was less than 0.1 % with the thermal expansion corrections described in the following section. The uncertainty of the density can be traced to the equation of state, as well as the pressure and temperature measurements made at the test section. The pressure measurements have an expanded uncertainty of 0.12 % and the expanded uncertainty in the calibration of the RTD's is 0.3 %. The average temperature of the flow was calculated by an area weighted quadrature formula using the three RTD's installed at the top, middle, and bottom of the pipe. Temperature stratification leads to greater uncertainty in the average temperature measurement for lower flows and higher temperature set points. A plot of the uncertainty of the volumetric flows used as the standard, reflecting the greater average temperature uncertainties for the high temperature tests is given in Fig. 3. The relative expanded uncertainties are nominally 0.8% except at the lowest three flows, where temperature stratification leads to V_B relative expanded uncertainty as high as 3.4 % for the 444 K test. The uncertainties at room temperature are smallest and remain about 0.7 % even at the lowest flows (no stratification).

THERMAL EXPANSION

Changes in the pipe area due to thermal expansion were taken into account using $\alpha = 15 \cdot 10^{-6}$ cm / (cm K) and $\Delta A = (2 \cdot \alpha \cdot \Delta T + \alpha^2 \cdot \Delta T^2)$. Over the 150 K temperature change of the tests, thermal expansion results in cross sectional area (and mean velocity) changes of 0.45 %.

¹ Standard conditions are 273.15 K and 101325 Pa.

² Volume or mole fraction.

³ All uncertainties are 95 % confidence level values, coverage factor $k = 2$, Taylor and Kuyatt (1994).

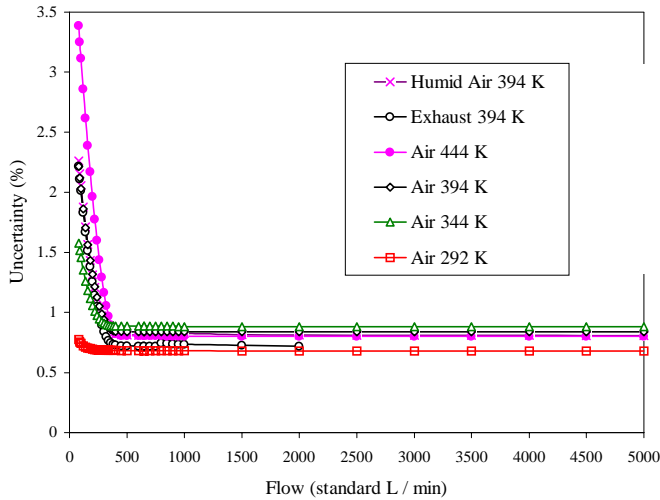


Figure 3. Uncertainty of the bulk mean velocity values used as the reference values of the tests.

Unfortunately, predictions of the effects of thermal expansion on the acoustic path length, ℓ , are not as straightforward as the flow tube area corrections. A thermal correction would involve at least three different thermal expansion coefficients (the flow tube material, the sensor support materials, and the transducer materials) as well as temperature measurements at different locations in the assembly. A different design could alleviate the difficulties, but it is also possible to calibrate out the effects of temperature changes on the path length. Meter measurements of sound speed were gathered at each set point temperature (after the entire system had reached thermal equilibrium). The test was carried out at the highest flow set point where good measurements of the gas temperature can be made (stratification is negligible). The sound speed values calculated by the meter using a constant path length were compared to handbook values for the sound speed at the measured temperature (Hilsenrath et al., 1955). The handbook and meter sound speeds can be used to form a factor, k_T , which corrects for the effects of thermal expansion on the path length as a function of temperature.

$$k_T = \frac{\left(\frac{c_H^T}{c_H^0} \right)}{\left(\frac{c_m^T}{c_m^0} \right)} \quad (5)$$

Such a correction was applied to all of the flowmeter data collected and it was as large as 0.8 % for the 150 K temperature change.

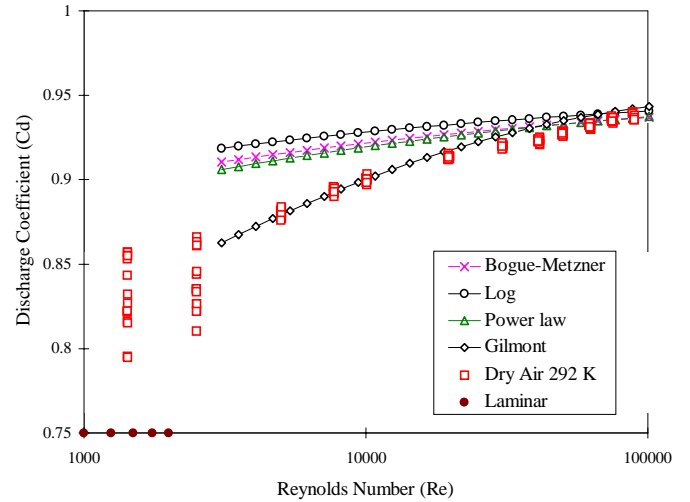


Figure 4. Discharge coefficient for analytical profile functions along with the 292 K experimental results.

RESULTS AND DISCUSSION

Figure 4 presents the 292 K experimental data along with the C_d predictions from analytical profile functions. The Gilmont profile matches the experimental data best, particularly for the low Reynolds number conditions. The worst disagreement between the Gilmont predictions and the experimental values is 0.86 % at $Re = 40\,000$.

Figures 5 and 6 show semi-log plots for all of the test conditions in dimensional and non-dimensional forms. (Points at flows < 100 liters / min have been removed from Fig. 5 for scaling convenience). From these figures it is clear that the discharge coefficient and Reynolds number effectively collapse the calibration data for a wide range of flow conditions. The plots show the individual 30 second averages, so there are 10 points at each test condition. For $Re > 4000$, Reynolds number scaling reduces the data scatter by a factor of two.

In Fig. 6, one can see that for Re between 5000 and 10 000, the 292 K data has much less scatter than the heated data points (1 % vs. 3 %). However, the two 292 K data sets at Re of 1500 and 2500 show scatter of over 5 %, due to transition or the laminar profile shape changing over time. The heated tests show greater scatter than the room temperature data due to unsteady temperature and velocity profiles caused by temperature stratification in the flow. As the Reynolds number falls below 10,000, mixing within the flow drops, and buoyancy leads to higher temperatures at the top of the pipe than at the bottom. Temperature stratification occurs once the Reynolds number is low enough that buoyancy forces are significant when compared to the axial inertial forces of the flow. Buoyancy forces lead to distortion of the velocity profile as well.

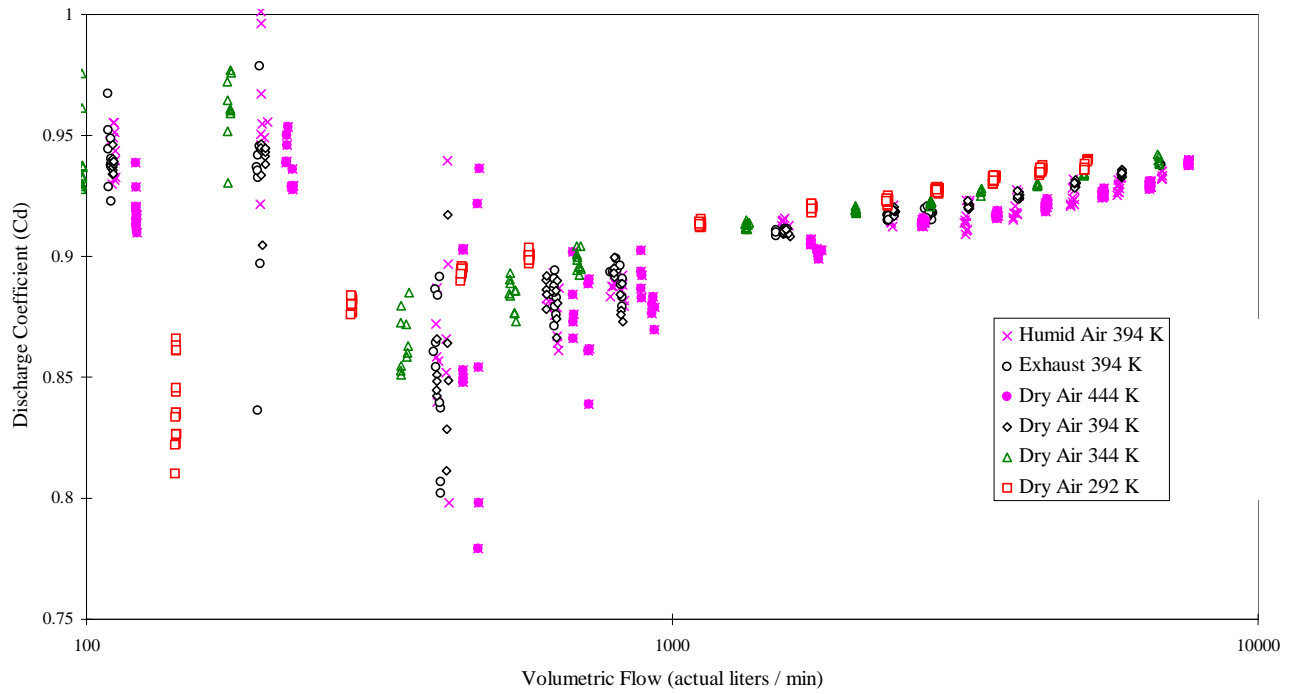


Figure 5. Semi-log plot of dimensional results: discharge coefficient versus flow for all test conditions.

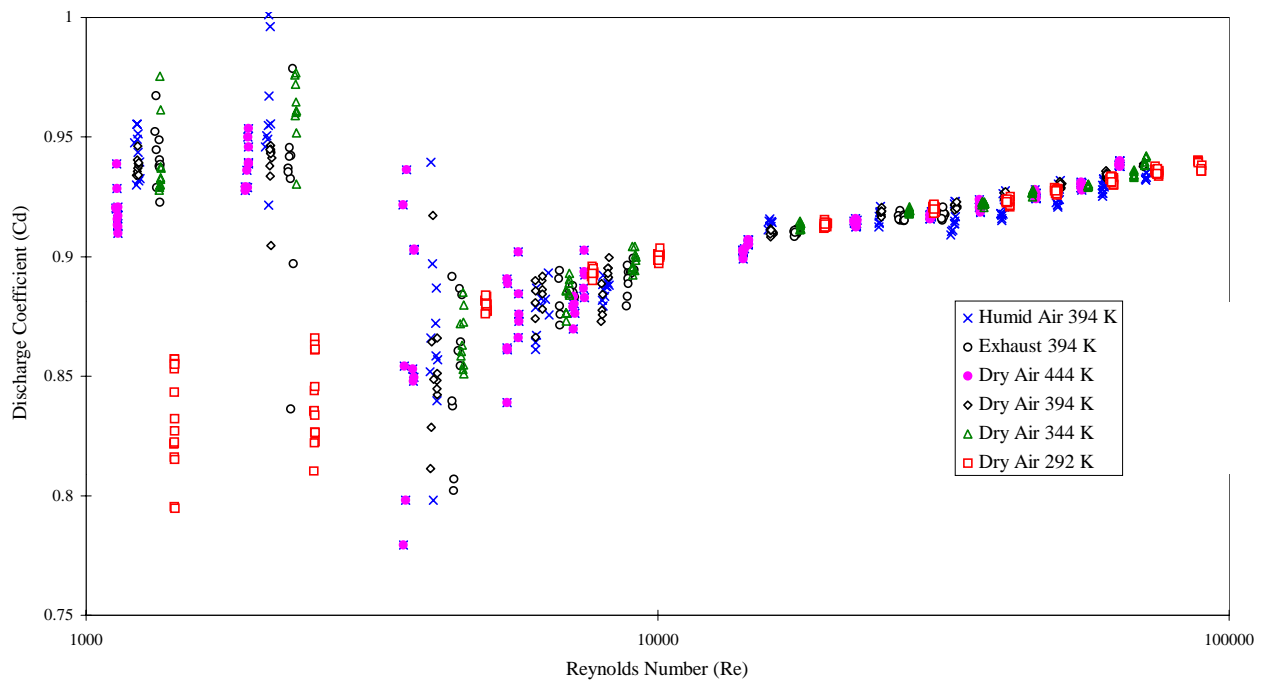


Figure 6. Semi-log plot of non-dimensional results: discharge coefficient versus Reynolds number for all test conditions.

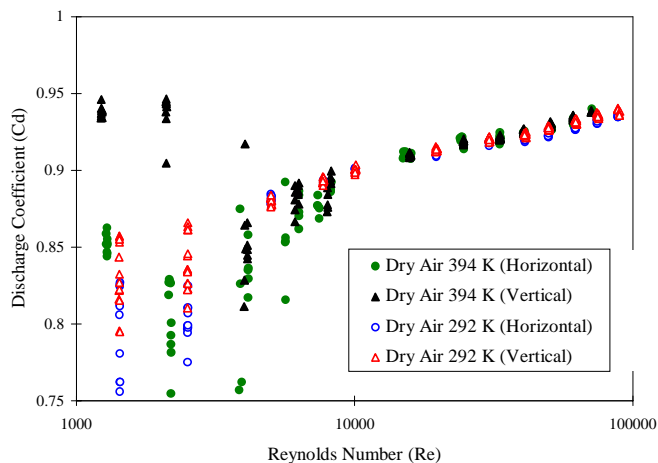


Figure 7. 292 K and 394 K results for horizontal and vertical sound path orientations.

Once the Reynolds number passes through transition to the laminar flow regime, the mixing drops further and temperature stratification becomes even more extreme. For the heated tests, at these lowest Reynolds numbers, the velocity profile is asymmetrical and C_d departs dramatically from the predictions computed for the “ideal” analytical profiles as well as the 292 K results. To prove that profile distortion was the cause of the C_d departure for $Re < 4000$, the meter was rotated 90° so that the sound path fell in the horizontal plane (instead of the vertical plane). While the 292 K behavior was nominally the same for both meter orientations, data at 394 K data showed much higher discharge coefficients for $Re < 10\,000$ (Fig. 7), demonstrating that the 292 K profile is essentially axisymmetric, while the 394 K profile is not.

Figure 8 presents the temperature stratification measured by the three RTD’s positioned at the top, middle, and bottom of the pipe for various Reynolds numbers at the three heated temperature set points. The stratification data is given as the difference between the top and bottom RTD’s as a percent of the average temperature at the test section. As expected, stratification increases with the temperature set point. The stratification was particularly great for the two lowest Reynolds numbers tested (1100 and 1900) since the mixing within the laminar flow is low. The figure shows that for the 444 K test at $Re = 1100$, the temperature stratification was 16 %. Time traces of the temperature data have been examined for the heated tests, and it can be seen that in some cases the temperature profile did not reach equilibrium after more than 30 minutes. Clearly the temperature stratification and the corresponding velocity profile distortions reach steady state very slowly.

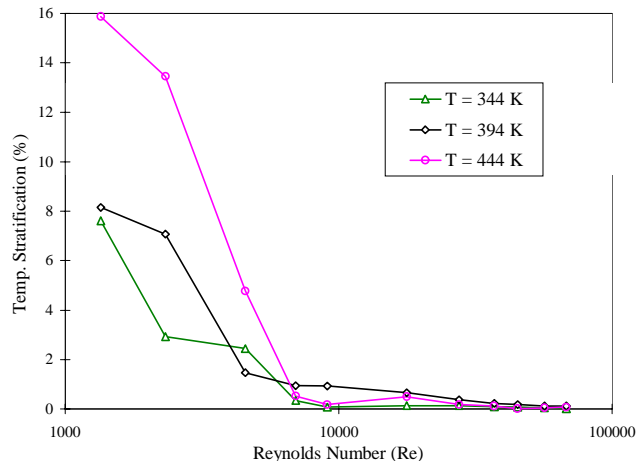


Figure 8. Temperature stratification (as a percent of the average temperature at the test section) versus Reynolds number for the three heated test conditions.

CONCLUSIONS

A transit time flowmeter has been tested over a wide range of gas property conditions. Transit time flowmeters are suitable for application in hot gas mixtures. However, the effects of profile shape and thermal expansion must be considered.

In these experiments, it has been shown that the discharge coefficient and Reynolds number effectively collapse transit time flowmeter calibration data. Therefore, the discharge coefficient and Reynolds number can be used to correct for the effects of profile shape on meter output for a particular meter piping arrangement. Using the dimensionless quantities improves the scatter in the calibration data sets by a factor of two.

Applying a discharge coefficient that is a function of Reynolds number would improve transit time flowmeter accuracy, particularly at Reynolds numbers below 30 000, where the change in C_d with respect to Re is relatively large. If the gas composition is known, the flowmeter measurements of sound speed can be used to calculate the gas temperature. The gas composition, temperature, path mean velocity, and a pressure measurement are the inputs necessary to calculate a Reynolds number. Therefore, it is practical to implement the described calibration improvements within commercial flowmeter electronics.

In this study, it has been found that the effects of thermal expansion on the pipe cross sectional area and on the sound path length are significant. For the 150 K temperature range in these tests the effects were 0.45 % and 0.80 % respectively. A simple method for measuring the path length changes as a

function of temperature using the meter sound speed determinations has been described. The designers of flow tubes and transducer holders should be cognizant of the thermal expansion issues so that the expansion can be predicted analytically or accurately extrapolated to more extreme temperatures. Also, the designs should be as repeatable as possible through many temperature cycles so that the path length does not creep and lead to calibration drift.

The discharge coefficient predictions based on the Gilmont profile best match the experimental results. The Gilmont predictions show the sharpest decline in discharge coefficient with decreasing Re .

At $Re < 10\,000$, the heated tests showed significantly more data scatter than the room temperature tests, due primarily to significant temperature stratification between the top and the bottom of the flow tube becomes significant. For laminar flows, the temperature stratification and velocity profile distortion become so severe that large departures from the room temperature behavior are observed (11 %). For the heated test conditions and the lowest flows, the temperature and velocity profiles did not reach steady state even after more than 30 minutes. The use of flow conditioners and orienting the meter so that the gas flows vertically instead of horizontally should reduce the effects of heat transfer and stratification on the flowmeter performance.

ACKNOWLEDGMENTS

The author would like to acknowledge the thoughtful assistance of Dr. T. T. Yeh.

REFERENCES

- Bogue, D. C. and Metzner, A. B., 1963, "Velocity Profiles in Turbulent Pipe Flow," *I&EC Fundamentals*, Vol. 2, No. 2.
- Brown, A. E., 1991, "Ultrasonic Flowmeters" in "Flow Measurement: Practical Guides for Measurement and Control," D. W. Spitzer, ed., Instrument Society of America, Research Triangle Park, NC, pp. 415.
- Gilmont, R., 1996, "Velocity Profile of Turbulent Flow in Smooth Circular Pipes," *Measurements and Control*, pp. 96-103.
- Hilsenrath, J. et. al., 1955, "Tables of Thermal Properties of Gases," NBS Circular 564.
- Lynnworth, L. C., 1989, "Ultrasonic Measurements for Process Control: Theory, Technique, Applications," Academic Press, San Diego, CA.

Taylor, B. N. and Kuyatt, C. E., "Guidelines for Evaluating and Expressing the Uncertainty of NIST Measurement Results," NIST Technical Note 1297, 1994.

Wright, J. D. and Espina, P. I., 1997, "Flowmeter Calibration Facility for Heated Gas Mixtures," National Conference of Standards Laboratories Proceedings, Atlanta, Ga., July, 1997, pp. 401-420.

Yeh, T. T. and Mattingly, G. E., 1997, "Computer Simulations of Ultrasonic Flowmeter Performance in Ideal and Non-Ideal Pipeflows," 1997 ASME Fluids Engineering Division Summer Meeting, June 22 - 26.